Aerosol and Air Quality Research, 15: 2277–2290, 2015

ISSN: 1680-8584 print / 2071-1409 online
doi: 10.4209/aaqr.2015.03.0153

Seasonal Variation and Chemical Characteristics of Atmospheric Particles at Three Islands in the Taiwan Strait

Tsung Chang Li[1], Chung Shin Yuan[1,3*], Kuo Cheng Lo[2], Chung Hsuang Hung[2†], Shui Ping Wu[3], Chuan Tong[4]

[1] *Institute of Environmental Engineering, National Sun Yat-sen University, Kaohsiung, Taiwan*
[2] *Department of Safety Health and Environmental Engineering, National Kaohsiung First University of Science and Technology, Kaohsiung, Taiwan*
[3] *College of Ecology and Environment, Xiamen University, Xiamen, China*
[4] *School of Geographic Science, Fujian Normal University, Fujian, China*

ABSTRACT

The seasonal variation and spatial distribution of atmospheric particles at three islands in the Taiwan Strait were investigated. Atmospheric particles (PM_{10}) were collected at three offshore islands (i.e., Kinmen islands, Matsu islands, and Penghu Islands) and two coastal regions (i.e., Xiamen and Fuzhou) in the years of 2008–2012. Field sampling results indicated that the average PM_{10} concentrations at the Kinmen islands were generally higher than other sampling sites, suggesting that a superimposition phenomenon was regularly observed during the air pollution episodes at Kinmen Islands and Xiamen region. PM_{10} samples were analyzed for their chemical composition, including water-soluble ions, metallic elements, and carbonaceous content. The most abundant water-soluble ionic species of PM_{10} were recognized as SO_4^{2-}, NO_3^-, and NH_4^+, indicating that PM_{10} was mainly composed of secondary inorganic aerosols. Although natural crustal elements dominated the metallic content of PM_{10}, the most abundant anthropogenic metals of PM_{10} were Zn and Pb. Enrichment factor calculations showed that Ni, Cr, and Zn were the enriched elements emitted mainly from anthropogenic sources. Moreover, the OC concentration of PM_{10} was always higher than that of EC at all sampling sites. High OC/EC ratios of PM_{10} were commonly observed at the sampling sites on the Matsu Islands, the Fuzhou region, and the Penghu Islands. Source apportionment results indicated that vehicular exhausts were the main source of PM_{10}, and followed by industrial boilers, secondary aerosols, soil dusts, biomass burning, petrochemical plants, steel plants, oceanic spray, and cement plants at the island and coastal sampling sites in the Taiwan Strait.

Keywords: Atmospheric particles in the Taiwan Strait; Superimposition phenomenon; Chemical characteristics; Spatiotemporal distribution; Source apportionment.

INTRODUCTION

The Taiwan Strait, located between Taiwan and mainland China, is one of the busiest marine transportation routes worldwide. Large quantities of anthropogenic particulate pollutants are emitted from the densely populated urban and thriving industrial areas to the west and east banks of the Taiwan Strait. The west bank of the Taiwan Strait covers the areas at the coastal region of Fujian Province, while the east bank covers the areas at the west coastal region of the Taiwan Island. Both the west and east banks of the Taiwan Strait were densely populated and thriving industrial areas, which emit huge amount of particles transported toward the Taiwan Strait via atmospheric dispersion. Major metropolitan areas are Xiamen and Fuzhou in the west bank, and Taipei, Taichung, and Kaohsiung in the east bank of the Taiwan Strait.

The impacts of Asian duststorms, biomass burning, and Asian haze on ambient particulate air quality commonly occur in spring and winter, when large quantities of natural and anthropogenic air pollutants are driven toward and across the Taiwan Strait. Three major islands, including Matsu Islands, Kinmen islands, and Penghu islands, located in the Taiwan Strait may have significant difference in the chemical composition of atmospheric particles in four seasons.

The Matsu Islands are located at the Minjiang Estuary at the northwestern Taiwan Strait, facing Fuzhou City in the

* Corresponding author.
Tel.: 886-7-5252000 Ext. 4409; Fax: 886-7-5254409
E-mail address: ycsngi@mail.nsysu.edu.tw
† Corresponding author.
Tel.: 886-7-6011000 Ext. 2320; Fax: 886-7-6011061
E-mail address: jeremyh@nkfust.edu.tw

Southeast China. The Matsu Islands have an annual average temperature of 18.4°C, scare and unevenly distributed rainfall, and the prevailing winds from the Northeastern Monsoons (from October to April of next year) and the Southwestern Monsoon (from May to August). The Matsu Islands consist of 36 small islands divided into four major townships, covering the entire areas of 29.51 km^2. The islands have no large-scale industries and emission sources, which qualifies the islands as a background environment. The Kinmen islands located at the Xiamen Bay in the southwestern Taiwan Strait, facing Xiamen City. The Kinmen islands have subtropical monsoon weather with an annual average temperature of 21.0°C, an annual rainfall of 1,043 mm, and the prevailing winds from the northeast (from fall to spring of next year) and the southwest (from May to August). The Kinmen Islands cover two major islands and several separately distributed small islands with a total area of 150.0 km^2. Kinmen islands have a few industrial sources, including an oil-fired power plant, ceramic plants, and distillery. But, there are plenty of industrial plants surrounding the Xiamen Bay in the mainland side, which might emit huge amount of particles from coal-fired power plants, stone processors, ceramic plants, porcelain products, and textile industrial. These particles could be blown and transported across the Xiamen Bay to the Kinmen Islands, resulting in high PM_{10} concentrations. Major industrial sources surrounding the Xiamen Bay are illustrated in Fig. S-1.

The Penghu Islands are offshore islands located at the southeastern Taiwan Strait, facing the southwestern coast of the Taiwan Island. The Penghu Islands have a total area of 128.0 km^2, which has the subtropical weather being mainly influenced by East Asian Monsoons. The potential sources at the Penghu islands include an oil-fired power plant, construction sites, and vehicular exhausts.

In winter and spring, the prevailing winds were blown northeasterly during the period of the Northeastern Monsoons in the Taiwan Strait. The contributions of long-range transportation dominated at the Penghu islands, followed by the Matsu Islands and the lowest at the Kinmen islands. There were very few local sources at the Penghu islands. PM_{10} was mainly transported from the coastal regions of China, Korean Peninsula, or Japan Islands toward the Penghu Islands (Lin *et al.*, 2004). Previous studies reported that cyclonic air circulation was generally observed at the Xiamen Bay due to the topography of Bay Area, which inhibited the dispersion of PM_{10} (Li *et al.*, 2013a). Although both long-range transport and local emissions were the main causes for the accumulation of atmospheric particles at the Xiamen Bay, the contribution of local emissions was generally higher than that of long-rang transport. The Matsu Islands were located at the northern Taiwan Strait. The contribution from long-range transport was generally higher than that of local emissions. For the past few years, the ambient air quality of the Matsu and the Kinmen Islands deteriorated gradually, and PM_{10} is responsible for the poor ambient air quality particularly in spring and winter. According to previous field monitoring data, high levels of PM_{10} (> 125 μg m^{-3}) found at the Kinmen Islands during the Northeastern Monsoon periods are likely blown from the northern upwind sources, suggesting that a superimposition phenomenon was regularly observed during the air pollution episodes in the Kinmen and Xiamen regions. The high PM_{10} concentrations observed at the Xiamen Bay were not only caused by long-range transport but also by local emissions, which was termed as "superimposition phenomenon". If the anthropogenic PM_{10} was blown northerly by long-range transport, higher PM_{10} concentrations should occur at the downwind sampling sites. However, field sampling results showed that the PM_{10} concentrations at the central area of the Xiamen Bay were higher than those at the upwind and downwind sites in the Xiamen Bay during the Northeastern Monsoons in spring and winter. Previous studies reported that high PM_{10} concentrations occurred in the Xiamen Bay were mainly caused by local emissions instead of long-range transport.

Local emissions from the Kinmen and Xiamen regions are thus more significant than those transported from a long distance by the Northeastern Monsoons (Li *et al.*, 2013a, b; We *et al.*, 2015). Previous results (Li *et al.*, 2013a, b) reported that the sampling sites located at the central area of Xiamen Bay had higher PM_{10} concentration than those at the upwind and downwind sites in the Xiamen Bay during the Northeastern Monsoons in spring and winter. It suggested that PM_{10} concentrations observed at the Xiamen Bay were not only caused by long-range transportation but also by local emissions. A superimposition phenomenon was regularly observed during air pollution episodes in the Xiamen Bay. Their results indicated that local emissions from the Xiamen Bay Area were more significant than long-range transport during the periods of the Northeastern Monsoons. The atmospheric particles at the Matsu Islands from June to August had the lowest concentrations in the whole year, the average monthly concentrations were lower than 50 μg m^{-3}, and rose from October to May of the sequential year. This phenomenon concurs closely with the change of wind direction, showing that wind direction is highly correlated with poor particulate air quality. The prevalence of the Northeastern Monsoons commonly occurred in winter and spring. The concentration of atmospheric particles at the Penghu Islands is always lower than the Ambient Air Quality Monitoring Stations in Taiwan. The highest PM_{10} concentrations were generally observed during the Asian duststorm periods, which deteriorated the ambient air quality from late winter to late spring.

Previous researches have investigated the seasonal variation and spatial distribution of ambient air pollutants by using the field measurement data obtained from the coastal stations of TAQMN (Chester *et al.*, 2000; Tsai *et al.*, 2008; Tsai *et al.*, 2010). TAQMN is an abbreviation of Taiwan Air Quality Monitoring Network (TAQMN) which was established by the Environmental Protection Administration of Taiwan since 1993. So far, the sampling of atmospheric particles has not been exerted at the offshore islands in the Taiwan Strait. The results revealed that the possible accumulation of air pollutants in the offshore and coastal regions causing air pollution episodes due to the combination of long-range transport and local emission sources has not been thoroughly investigated yet (Tsai *et al.*, 2010). In order

to ascertain the spatiotemporal variation and to characterize the chemical composition of atmospheric particles at the offshore islands and along the coastal region in the Taiwan Strait, three island sites and two coastal sites were selected for sampling PM_{10} in this particular study. This study aims to investigate the spatiotemporal variation and chemical characteristics of atmospheric particles (PM_{10}) around the coastal regions in the Taiwan Strait. Source identification and apportionment of atmospheric PM_{10} were further determined.

METHODS

Sampling Protocol

PM_{10} samples were collected at three island sites (i.e., Kinmen, Matsu, and Penghu) in the Taiwan Strait and two coastal sites (i.e., Fuzhou and Xiamen) (see Table S-1) along the western bank of the Taiwan Strait in the years of 2008–2012. The coastal sampling sites were located at the Fuzhou coastline and metro Xiamen, while the island sampling sites were located at the Matsu Islands, the Kinmen Islands, and the Penghu Islands. The locations of the island and coastal sites in the Taiwan Strait are illustrated in Fig. 1.

The coastal sampling sites in the Fuzhou areas have three sites located along the coastline of the Minjiang Estuary (see Fig. 1(a)), while the Xiamen sampling sites have five sites at metro Xiamen located around the Xiamen Bay (see Fig. 1(b)). Three sampling sites along the coastline of the Minjiang Estuary were located at Huangqi Junior high School (HQ), Baison High School (BS), and Meihua High School (MH). The coastal sampling sites located in metro Xiamen (XM) include the Xiamen University, Jinjing Elementary School, Anhai Elementary School, Xiangzhi Elementary School, Daderng High School. These coastal sites are mostly nearby a street and thus likely to be influenced by fine particles emitted from vehicular exhausts and/or industrial areas along the coastal region of Xiamen, which is surrounded by high-density industries, power plants, vehicular exhausts, and textile industries. Three sampling sites at the Matsu Islands include Nankan Meteorological Station (NK), Zhongshan Junior High School (BG), and Donyin Town Hall (DY). The Matsu islands' major stationary sources are thermal power plants, breweries, gas stations, and no industrial processes. Recognized as a national park, the Kinmen Islands' local emission sources are well controlled.

Air pollutants are mainly emitted from the upwind northern and northeastern industrial areas in the Jinjiang River Basin during the Northeastern Monsoon periods (Hsu *et al.*, 2010; Li *et al.*, 2013a, b). The sampling site at the Penghu Islands is located at the northwestern tip of the main island, named the Hsiao-men fishery village, in order to avoid local sources near the Makung City, the most populated area at the islands. The Hsiao-men sampling site is approximately 12 m above the ground and 500 m and 50 m far from the coastline and the major roads, respectively.

The sampling of PM_{10} was respectively conducted at the island and coastal sampling sites around the Taiwan Strait from 2008 to 2012. Twenty-four hour PM_{10} was collected by a high-volume sampler from 9:00 am to 9:00 am of the sequential day at each site. In this study, the sampling frequency of PM_{10} collected by high-volume samplers is summarized in Table S-2. Due to limiting financial support from Taiwan EPA and the shortages of human resources and PM_{10} samplers, the PM_{10} sampling could not be conducted simultaneously. The numbers of PM_{10} samples collected at these three islands were 750, 204, and 420, respectively,

High-volume samplers of same brand name were used to collect PM_{10} with the sampling flow rate of 1.4 m^3 min^{-1}. This sampling method was complied with the sampling method of NIEA A102.12A. Quartz-fiber filters used in this study are manufactured by Pall Corporation. Quartz filters were selected in this study since we are interested in the chemical composition of water-soluble ionic species, metallic elements, and carbonaceous content. Before weighing, the quartz-fiber filters were equilibrated in a desiccator at temperatures between 20°C and 25°C and relative humidities (RH) between 35% and 45% for forty–eight hours. After conditioning, the filters were then weighed by a microbalance with the precision of 1 μg to determine the PM_{10} mass. The moisture could be mostly removed in the process of conditioning (Cheng and Tsai, 2000; Yuan *et al.*, 2006).

Chemical Analysis

After PM_{10} sampling, the quartz fiber filters were temporarily stored at 4°C to conserve their chemical stability, and they were then sent back to a Air Pollution Laboratory which were the main laboratory responsible for chemical analysis of PM_{10} at National Sun-Yat Sen University for further chemical analysis. All quartz fiber filters were divided into four identical parts prior to the chemical analysis. One quarter of the quartz fiber filter was analyzed for water-soluble ionic species with an ion chromatography (DIONEX, Model DX-120). Major anions (F^-, Cl^-, SO_4^{2-} and NO_3^-) and cations (NH_4^+, K^+, Na^+, Ca^{2+} and Mg^{2+}) were further measured. An additional quarter of the quartz fiber filter was analyzed for the metallic content of PM_{10} with an inductively coupled plasma-atomic emission spectrometry (ICP-AES) (Perkin Elmer, Model Optima 2000DV). The metallic elements measured for this study included Na, Ca, Al, Fe, Mg, K, Zn, Cr, Ti, Mn, Ni, Pb, and Cu. Another quarter of the quartz fiber filters was used to determine the carbonaceous content of PM_{10}. Elemental, organic, and total carbons (OC, EC, and TC) were measured with an elemental analyzer (Carlo Erba, Model 1108). Prior to sampling, the quartz fiber filters were preheated at 900°C for 1.5 hours to expel carbon impurities from the filters. A quarter of each filter was heated in advance at 340°C for 100 min to expel organic carbon (OC) prior to carbon analysis. The heating time adopted herein (100 min) (Wang *et al.*, 2008) was in the between of that (340°C for 120 mins) adopted by Cachier *et al.* (1989) and that (340°C for 43 mins) used by Lavanchy *et al.* (1999). After which the amount of elemental carbon (EC) was determined. Another eighth of the quartz fiber filters was analyzed without heating to determine the total carbon (TC). The amount of organic carbon (OC) was then estimated by subtracting the EC from the TC.

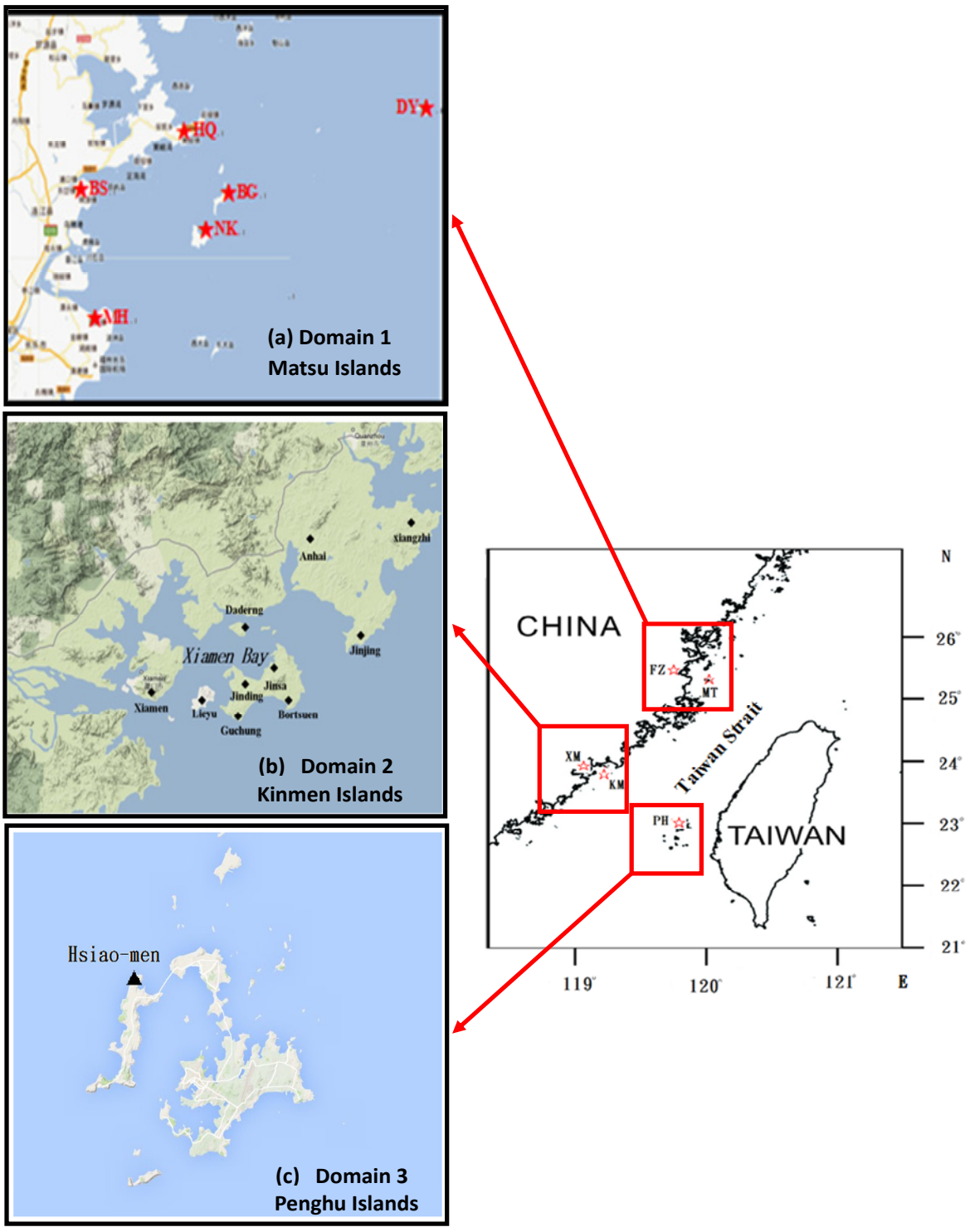

Fig. 1. Location of PM_{10} sampling sites at three target domains in the Taiwan Strait.

Quality Assurance and Quality Control

Quality assurance and quality control (QA/QC) for both PM_{10} sampling and chemical analysis were conducted in this study. Prior to PM_{10} sampling, the volumetric flow rate of each PM_{10} sampler was carefully calibrated with a film flow meter (SENSIDYNE MCH-01). The quartz filters were handled with care, so as to prevent potential cracking during the sampling procedures, as they were placed on the PM_{10} samplers. After sampling, aluminum foil was used to fold the quartz filters which were then temporarily stored at 4°C and transported back to the Air Pollution Laboratory for further chemical analysis. The sampling and analytical procedures were similar to those described in previous studies (Witz *et al.*, 1990; Cheng and Tsai, 2000; Lin, 2002; Yuan *et al.*, 2006; Tsai *et al.*, 2008; Tsai *et al.*, 2010).

Chemical Mass Balanced (CMB) Receptor Model

The source apportionment of ambient PM_{10} was assessed using a receptor model based on the principle of chemical mass balance (CMB) (Kothai *et al.*, 2008; Yatkin and Bayram, 2008; Li *et al.*, 2013; Shi *et al.*, 2014; Chen *et al.*, 2015). Since the detailed descriptions of CMB receptor model (e.g., CMB 8.0) are available elsewhere, only a brief summary is presented as supplementary file S1-1 and Table S-3. Ten major local source profiles (noted by * in Table S-3) obtained from previous studies were selected to conduct the source apportionment of PM_{10} in this study (Li *et al.*, 2013b). These sources surrounding the Xiamen Bay included stone processing, cement industries, ceramic plants, tile industries, coal burning, coal ash, fugitive dusts, biomass burning, construction dusts, and road dusts as shown in Table S-3.

WRF Model Operation and Domain Setting

Weather research and forecasting model (WRF V3.1) is a newly proposed meteorological model by NOAA/ESRL, which was used to simulate air flow fields in the investigated areas for this study. In comparison to the past models (such as MM5, Model 3, and SAQM), WRF produces a friendly environment for massively parallel computation by the improved characteristics of non-hydrostatic air flow fields and provides various choices for physical parameterizations (Jiang *et al.*, 2008; Kumar *et al.*, 2012; Lo and Huang, 2012; Huang *et al*., 2013; Shahid *et al.*, 2015). WRF is good for investigating regional-scale air flow field program analysis (Borge *et al.*, 2008; Peckham *et al.*, 2012). To simulate the air flow fields of the investigated areas, the WRF model was conducted for March 6th and Oct. 8th in 2013 and Apr. 11th in 2014, respectively. In addition, their initial 24-hour periods in advance were selected as pre-integration stages for the investigated cases. There were three domains, defined by Lambert projection and used for model simulation, applied for model operation, which are summarized in Tables S-4 and S1-2.

RESULTS AND DISCUSSION

Spatiotemporal Variation of PM_{10} Concentration

Fig. 2 illustrates the seasonal variation of ambient PM_{10} concentrations, which were generally higher in winter and spring than those in summer and fall at all sampling sites. More specifically, the PM_{10} concentrations at the XM and KM sites were mostly higher than those at other sampling sites. The PM_{10} concentrations ranged from 79.59 to 88.59 μg m^{-3} and from 94.83 to 120.24 μg m^{-3} at the KM and XM sites, respectively. Comparing the island site (KM) to the coastal site (XM), the PM_{10} concentrations at the XM site were 1.2 to 1.4 times than those at the KM site, indicating that the PM_{10} concentrations at the metropolitan Xiamen were relatively higher than those at the Kinmen Islands. According to the PM_{10} concentrations measured at different sampling sites in areas of Kinmen and Xiamen islands, the high PM_{10} concentrations were always observed at the sites adjacent to the industrial areas along the southeastern coast of Xiamen Bay. The PM_{10} concentrations in winter were always higher than those in summer, because the prevailing wind at the Xiamen Bay is dominated by Northeastern Monsoons in winter, which could blow particulate pollutants from the eastern coastal region of North mainland China, Korea Peninsula or Japan Islands to the Xiamen Bay. However, local emissions from the surrounding region of the Xiamen and Kinmen were as important as long-range transportation by Northeastern Monsoons, and thus a superimposition phenomenon was regularly and commonly observed during the air pollution episodes in Kinmen and Xiamen regions.

A similar trend of the PM_{10} concentrations was observed at the FZ and MT sampling sites. The PM_{10} concentrations at the FZ site were 1.1 to 1.5 times higher than those at the MT site. The PM_{10} concentrations observed at the FZ site were generally higher than the MT site for all seasons, showing that ambient PM_{10} at the Matsu Islands and the Fuzhou regions was not only influenced by long-range transport, but also by local emissions from the metropolitan Fuzhou. The level of atmospheric PM_{10} was highly influenced by meteorological condition, thus PM_{10} concentrations in spring, fall, and winter were much higher than those in summer. PM_{10} concentrations measured in summer were much lower than those in other seasons. In general, prevailing southerly or southwesterly breezes accompanied with clean marine aerosols were usually observed in summer, which observed in the warm afternoon in summer. Both contributed to the reduction of PM_{10} concentrations in the ambient air. Unlike other two investigated areas, the PM_{10} concentrations at the Penghu Islands (PH site) were very consistent for all seasons, because there were no large industrial sources in this region. The emission came mainly from the northern and northeastern China. The highest PM_{10} concentrations were observed during the Asian duststorm periods with a significant increase of atmospheric aerosols, particularly PM_{10}, and have been observed at the PH site, which commonly deteriorated the ambient air quality of the Penghu Islands from late winter to late spring. Compared to the island and coastal sites, the PM_{10} concentrations were always higher at the coastal sites than those at the island sites. Moreover, the highest PM_{10} concentrations were generally observed at XM and KM sites, which located at the southern Taiwan Strait, suggesting the anthropogenic emissions transported to northern Taiwan Strait by the Northeastern Monsoon. The PM_{10} concentrations were significantly increased at the southern Taiwan Strait. A superimposition phenomenon was regularly observed around the southern Taiwan Strait, which means local emissions and long-range transport were both important at the southern Taiwan Strait (Li *et al.*, 2013a). Long-range transportation from northeastern coastal regions of North mainland China Korea Peninsula, and Japan Islands were significantly might affected the ambient atmospheric at northern than those at the southern Taiwan Strait. Moreover, the highest PM_{10} concentrations of 154 μg m^{-3} at Matsu Islands, 170 μg m^{-3} at the Kinmen Islands, and 60 μg m^{-3} at the Penghu Islands, respectively, were observed on March 6th, 2013, April 11th, 2014, and October 8th, 2013. The air masses transported toward the above target islands were further interpreted by the simulated surface wind fields of these three spatial domains defined in this study.

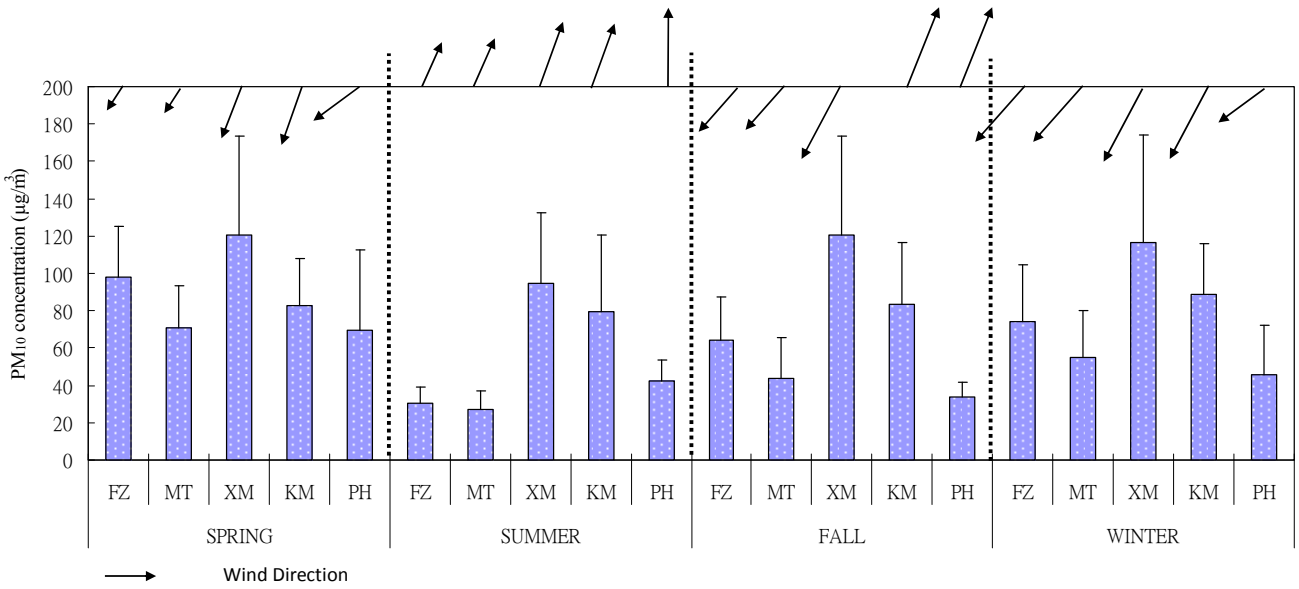

Fig. 2. Spatiotemporal variation of PM_{10} concentration at the island and coastal sampling sites in the Taiwan Strait. Summer was defined as June to August, Fall as September to November, Winter as December to February, and Spring as March to May for the sampling periods of 2008–2012.

Chemical Characteristics of PM_{10}

This study investigated the seasonal variation and chemical characteristic of atmospheric particles in the areas around the Taiwan Strait. Table S-5 summarizes the concentrations of atmospheric particles and their chemical composition at the island and coastal sampling sites in the Taiwan Strait. Fig. 3(a) illustrates the seasonal variation of ionic species of PM_{10} at the islands and coastal areas in the Taiwan Strait which were selected for this study. Chemical analysis of PM_{10} showed that the most abundant water-soluble ionic species were SO_4^{2-}, NO_3^-, and NH_4^+, indicating that secondary inorganic aerosols (SIA) were the major components of PM_{10}. The probable chemical compounds of PM_{10} were ammonium sulfate ($(NH_4)_2SO_4$) and ammonium nitrate (NH_4NO_3) (Yao *et al.*, 2003; Han *et al.*, 2007; Kocak *et al.*, 2007), which were originated from the neutralization of sulfuric and nitric acids with ammonium (Stockwell *et al.*, 2003). Table 1 summarizes the mass ratio of secondary inorganic aerosols to water-soluble ions and PM_{10} concentration (SIA/WSI and SIA/PM_{10}), respectively, during the sampling periods. The secondary inorganic aerosols accounted for 61.01–90.78% of WSI and 18.78–43.82% of $PM_{10,}$ respectively. The concentrations of SIA at the KM and XM sites were generally higher than those at the MT and FZ sites, and the PH site in the Taiwan Strait. At all sampling sites, the concentrations of SO_4^{2-} and NO_3^- were significantly higher at the FZ and XM sites located at the west-bank of the Taiwan Strait. It was speculated that the secondary SO_4^{2-} and NO_3^- were mainly attributed to the burgeoning industrial development in the coastal region of southeastern China. This suggested that anthropogenic emissions from southeastern China could migrate toward the XM, KM, FZ, and MT sampling regions in the Taiwan Strait during the Northeastern Monsoon periods. The percentages of water-soluble ionic species in PM_{10} at the PH site were generally the lowest compared to other four sampling sites in all seasons except in spring.

Previous studies used the extent of the neutralization of acidic sulfate and nitrate by ammonia to evaluate the acidic characteristics of atmospheric particles (Pathak *et al.*, 2009). A comparison of ammonium concentrations to non-sea salt sulfate plus nitrate concentrations ($[NH_4^+]/(nss\text{-}[SO_4^{2-}] + [NO_3^-])$, in the unit of micro equivalents per cubic meter ($\mu eq\ m^{-3}$) is shown in Fig. S-2. The microequivalent concentrations of SO_4^{2-}, NO_3^-, and NH_4^+ ($\mu eq\ m^{-3}$) were determined by dividing the mass concentration ($\mu g\ m^{-3}$) by its equivalent molecular weight. The nss-SO_4 is the excess sulfate that was calculated by subtracting the amount of SO_4^{2-} of marine from that of SO_4^{2-} in the atmosphere (Cheng *et al.*, 2000). We can then determine the nss-$[SO_4^{2-}]$ concentration by equation $nss\text{-}SO_4^{2-} = SO_4^{2-} - 0.251 \times Na^+$. The results showed that the neutralization ratios (NR) of PM_{10} were generally smaller than unity at all sampling sites, suggesting that atmospheric particles in these three targeted regions were mostly acidic. It is mainly affected by the transportation of acidic particles emitted from the up-wind sources at the Jinjiang River Basin (Hsu *et al.*, 2010; Li *et al.*, 2013a, b).

Fig. 3(b) illustrates the metallic content of PM_{10} sampled at the island and coastal sampling sites in the Taiwan Strait. Crustal elements (Ca, Mg, Fe, and Al) contributed the major metallic content of $PM_{10,}$ while the concentrations of trace metals (Cd, As, Ni, and Cr) increased during the Northeastern Monsoon periods, showing that Northeastern Monsoons could bring atmospheric particles with high content of trace metals emitted from multiple sources. The concentrations of Ca and Fe observed at the FZ site over the rural open lands were mostly higher than those at the MT site. Moreover, Al and Ca are the main elements in the earth's crustal coarse dusts mainly emitted from cement

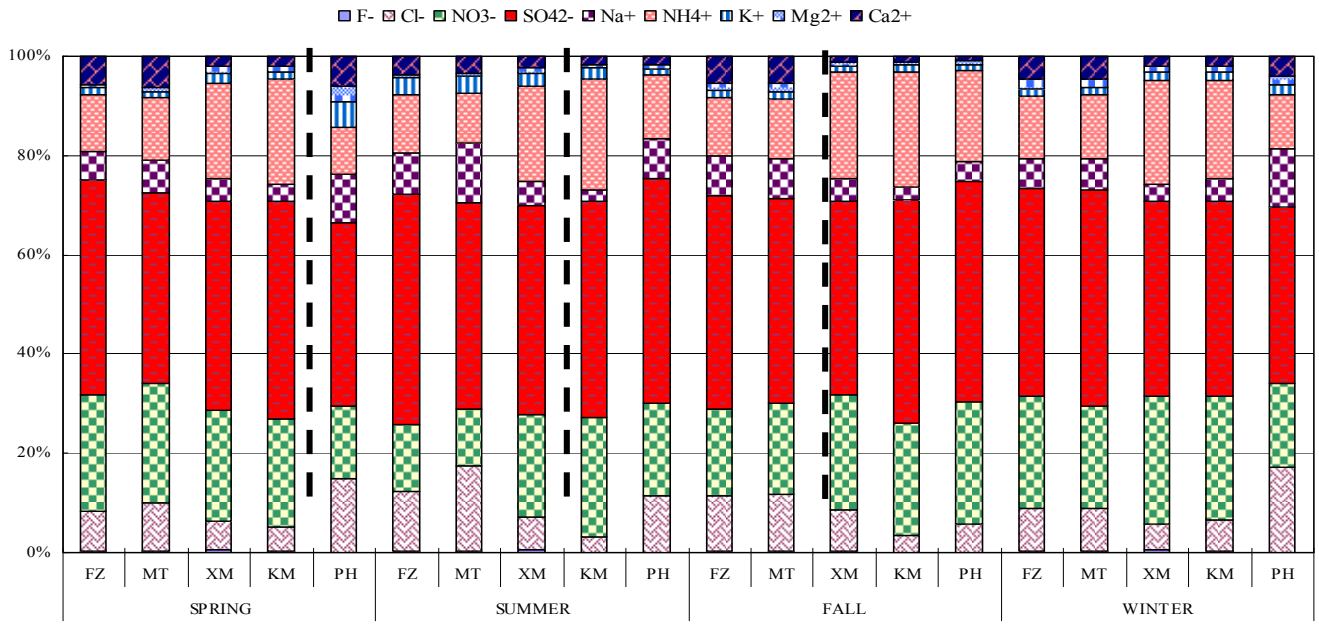

Fig. 3(a). Spatiotemporal variation of ionic concentration of PM_{10} sampled at the island and coastal sampling sites in the Taiwan Strait.

Table 1. The mass ratio of secondary inorganic aerosols (SIA) to water-soluble (WSI) and PM_{10} concentration at all sampling sites during the sampling periods.

Season	Sampling Sites	SIA/WSI (%)	SIA/PM_{10} (%)
Spring	FZ	78.20	28.33
	MT	75.17	30.50
	XM	83.85	27.64
	KM	87.04	37.37
	PH	61.01	31.09
Summer	FZ	71.82	23.97
	MT	62.98	21.88
	XM	81.69	43.82
	KM	89.85	39.26
	PH	76.67	18.78
Fall	FZ	72.26	28.25
	MT	71.41	26.20
	XM	83.46	32.28
	KM	90.78	38.61
	PH	87.10	21.00
Winter	FZ	76.95	30.59
	MT	76.90	26.85
	XM	85.80	35.33
	KM	84.10	33.43
	PH	63.21	21.58

Secondary Inorganic Aerosols (SIA) = NO_3^- + SO_4^{2-} + NH_4^+; WSI: Water-soluble Ions.

plants, road dusts, and the wind-blown dusts. Anthropogenic metallic elements could be transported to the Minjiang Estuary from urban and industrial sources in the northern mainland China, Korean Peninsula or Japan Islands through long-range transportation by the Northeastern Monsoons. Among these crustal elements, Al, Ca, and Fe were the most abundant metals, with much higher concentrations of Al than other crustal elements, especially at the PH sampling site. Al and Ca come mainly from cross-boundary wind-blown dusts and local fugitive dusts emitted from construction sites; both of which could significantly increase the loading of atmospheric particles (Huang *et al.*, 1994; Li *et al.*, 2013a). The concentrations of Ca and Fe at the XM sites were generally higher than those at the Kinmen sites, suggesting they came mainly from rural open lands, construction, stone processing plants located at the north coastline of the Xiamen Bay.

In contract, the concentrations of anthropogenic elements (Zn, Ni and Pb) at the XM and KM sites were always higher than those at the MT, FZ, and PH sites. Zn and Pb were the major trace components among the anthropogenic elements. Moreover, anthropogenic metallic elements could be transported to Xiamen Bay from the eastern coast of mainland China, Korean Peninsula or Japan Islands through long-range transportation by the Northeastern Monsoons. Previous studies reported that the high number of vessels navigating through the Taiwan Strait could result in high Zn and Pb emissions (Li *et al.*, 2013a). Oil burning on heavy vessels is the major source of Pb in the ocean, which makes it a good trace marker for vessel emissions. In addition to vessel exhausts, Pb could be emitted from municipal and industrial waste incinerators (Nriagu, 1988; Pirrone *et al.*, 1996).

The highest concentrations of Al were observed at the PH site in the season of spring, suggesting that atmospheric particles might came from Asian duststorms, which blew a huge amount of natural mineral dusts toward the southern Taiwan Strait from Inner Mongolia. Previous studies have commonly used Al and Fe as the reference elements for crustal particles in the Enrichment Factor (EF) calculations. The results showed that the chemical compositions of

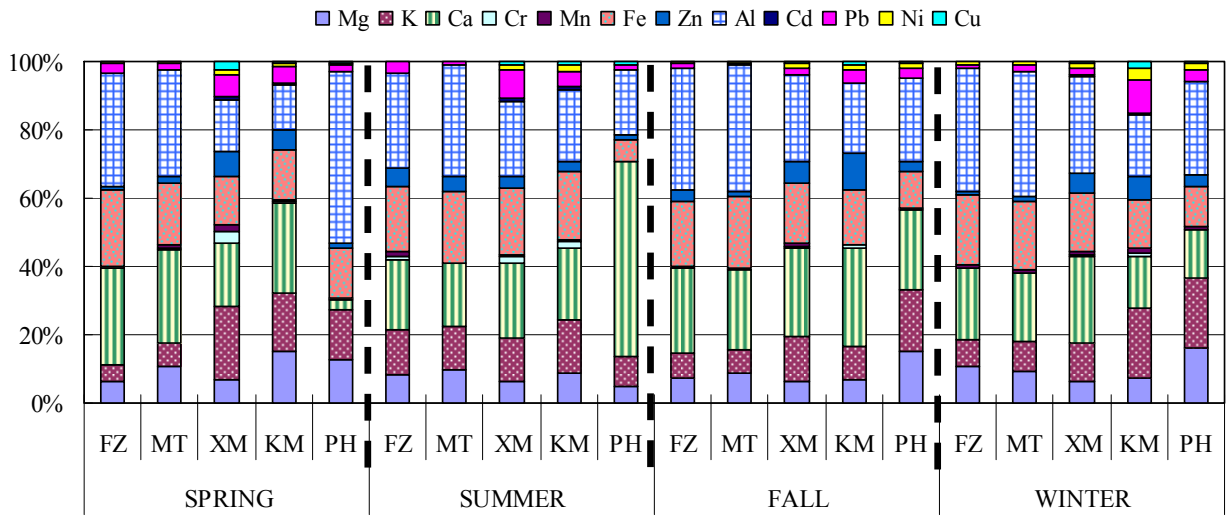

Fig. 3(b). Spatiotemporal variation of metallic concentration of PM_{10} sampled at the island and coastal sampling sites in the Taiwan Strait.

atmospheric particles sampled at the Penghu Islands were very much similar to the soil dusts emitted from the Inner Mongolia (Jen *et al.*, 2014).

Atmospheric organic carbons (OC) are emitted as primary aerosols directly from original sources as well as atmospheric photochemical reactions through the oxidation of volatile organic compounds (VOCs) via gas-to-particle conversion (Pandis *et al.*, 1992). However, atmospheric elemental carbons (EC) originated predominantly from the incomplete combustion such as fossil fuel combustion and biomass burning. Consequently, the relationship between OC and EC concentrations can reflect the origin of carbonaceous particles (Turpin and Huntzicker, 1991, 1995). The correlation between OC and EC is expected to be high if major fractions of OC and EC are emitted from a dominant primary source (Na *et al.*, 2004). As EC is a stable species against the oxidation occurred in the atmosphere, it is a very good tracer of primary anthropogenic sources and has been widely applied to estimate the concentrations of secondary organic compounds (SOC) (Feng *et al.*, 2009; Lin *et al.*, 2009). The EC tracer method assumes primary OC (POC) comes from the same combustion sources with EC. If the primary OC/EC ratio ($(OC/EC)_{pri}$) is available, we can then determine the SOC concentration by equation (1),

$$SOC = OC - EC \times (OC/EC)_{pri} \quad (1)$$

However, the $(OC/EC)_{pri}$ is a source- and seasonal-specific parameter, and is also affected by the carbon determination method (Khan *et al.*, 2012). The observed minimum OC/EC ratio at a specific sampling site was often used to represent the $(OC/EC)_{pri}$ on the assumption that the meteorological conditions are not favorable for the SOC formation during the sampling periods (Turpin and Huntzicker, 1995). This study estimated the primary OC/EC ratio ($(OC/EC)_{pri}$) determined as the smallest ratio of particulate OC to EC in each season at all sampling sites, representing the primary OC and EC of PM_{10} (Millet *et al.*, 2005; Hu *et al.*, 2012).

Fig. 3(c) illustrates the spatiotemporal variation of carbonaceous contents and their mass ratios (OC/EC) of PM_{10} sampled at the island and coastal sites in the Taiwan Strait. Primary organic carbons (POC) are emitted from anthropogenic sources, while secondary organic carbo (SOC) are formed by chemical reactions in the atmosphere. Elemental carbon (EC), which has a chemical structure similar to that of pure graphite, originates primarily from the direct emissions of fuel combustion and waste incineration. The concentrations of OC in PM_{10} at the island sites in the Taiwan Strait were always higher than those of EC for all seasons. The mass ratios of OC to EC (OC/EC) ranged from 2.0 to 3.0 at the MT, FZ, and PH sampling sites, and from 1.5 to 2.0 at the KM and XM sampling sites. The highest OC and EC concentrations of PM_{10} were both observed at the XM site, which was adjacent to major stationary sources, such as petrochemical plants, industrial complexes, and direct emissions of fuel combustion. The OC/EC ratios were always higher than 2.2 for PM_{10} at the FZ, MT, and PH sampling sites, showing that there were secondary organic aerosols formed in the Minjiang Estuary (Turpin *et al.*, 1990; Hildemann *et al.*, 1991). Under certain meteorological conditions (e.g., Northeastern Monsoons), emissions of huge amounts of volatile organic compounds (VOCs) from various sources (e.g., textile industry at the Jinjing River Basin) contribute to the formation of secondary organic aerosols (Hsu *et al.*, 2010). The OC/EC ratio has been used in other studies to clarify whether the carbonaceous aerosols are primary or secondary. A high OC/EC ratio coupled with a poor correlation implies an influx of urban pollutants from elsewhere or the secondary OC formed from atmospheric reactions. On the other hand, a high correlation indicated primary emissions and secondary carbon formation derived from primary carbons (Turpin and Huntzicker, 1995; Strader *et al.*, 1999).

Fig. S-3 illustrates the seasonal variation of the estimated secondary OC concentration and their contribution to the total OC (SOC/OC) of PM_{10} sampled at the island and coastal

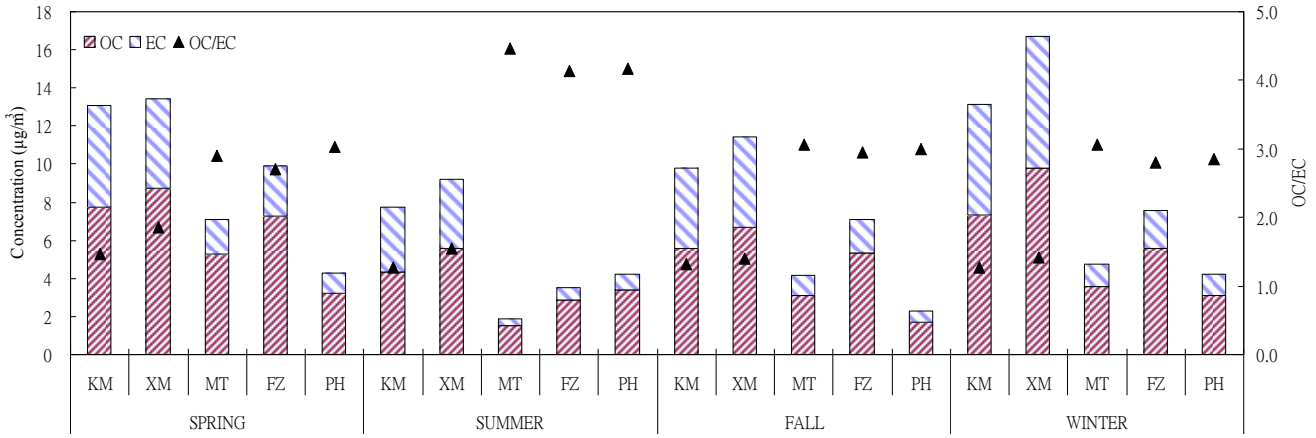

Fig. 3(c). Spatiotemporal variation of carbonaceous concentration and their mass ratios (OC/EC) of PM_{10} sampled in the Taiwan Strait.

sampling sites in the Taiwan Strait. The concentrations of secondary organic carbons (SOC) were estimated using the EC-tracer method (Turpin and Huntzicker, 1991). Moreover, the primary OC to EC ratio, $(OC/EC)_{primary}$, was simplified as the smallest ratio of particulate OC to EC $(OC/EC)_{min}$ in each season. The concentrations of SOC and OC on each sampling day are shown in Fig. S-3. A similar trend of concentrations of OC and the highest average concentrations of SOC were observed at the FZ, MT, and PH sampling sites, while the highest ratio of SOC/OC occurred at the PH (0.60) and MT sampling sites (0.53), respectively, in summer.

Source Apportionment of PM_{10}

Table 2 summarizes the source apportionment of PM_{10} collected at all sampling sites in this study, and an obvious seasonal variation was observed. According to the results of source apportionment, vehicular exhausts were the main source of PM_{10} at the XM, KM, FZ, and MT sampling sites, and followed by industrial boilers, secondary aerosols, soil dusts (including road dusts), biomass burning, petrochemical plants, steel plants, oceanic spray, and cement plants at the sampling sites. Among these, soil dusts, vehicular exhausts, petrochemical plants, and industrial boilers were the major sources in metro Xiamen, whereas soil dusts and biomass burning dominated in the Kinmen Islands. The contribution of vehicular exhausts to PM_{10} in metro Xiamen was always higher than that at other sampling sites, since metro Xiamen has the heaviest traffics compared to other areas. Although vehicular exhausts were the dominant source, biomass burning and secondary aerosols were also significant sources causing an increase in PM_{10} at urban and suburban areas. In winter, the Northern Monsoons transported suspended particles from the upwind emission sources (e.g., Jinjiang River Basin) to the downwind sites on Kinmen Islands, causing a significant increase in secondary inorganic aerosols mainly composed of sulfate and nitrate. Moreover, the contribution of secondary aerosols to PM_{10} in metro Xiamen was generally higher than that in the Kinmen Islands. In contrast, the contribution of biomass burning to PM_{10} in the Kinmen Islands was commonly higher than that in metro Xiamen.

The source apportionment of PM_{10} at the MT and FZ sampling sites located at the northwestern Taiwan Strait indicated that soil dusts, sea salts, secondary aerosols and vehicular exhausts were the main sources of PM_{10}. Sea salts at the offshore island sites contributed 3–10% more than those at the coastal sites, and increased significantly during the northeasterly winds. Soil dusts at the coastal sites in the Minjiang Estuary contributed about 2–11% more than those at the offshore island sites. The contribution of biomass burning rose significantly as high as 7% of PM_{10} in fall and winter, reflecting the open burning of agricultural debris in most areas of the Minjiang Estuary. It is noteworthy that, during the Northeastern Monsoon periods, polluted air mass transported mostly from the north due to the influence of high pressure anticyclone system centered at the Mongolian Plateau. The air masses originated from the north mainland China, Korean Peninsula, or Japan Islands passed through major industrial developing cities along the coastal regions of eastern China's coastal zone (Hsu *et al.*, 2010).

Surface Wind Fields of Three Domains in the Taiwan Strait

In order to figure out the surface wind field, an analysis of the weather (synoptic) charts near the land's surface was carried out in this study. As the weather charts provide data on the atmospheric state (i.e., on the distribution and characteristics of air masses, the atmospheric fronts, the different baric systems such as cyclones, anticyclones, troughs, crests, etc.,), a synoptic analysis allowed us to follow the changes in the evolution of weather systems in the investigation regions.

There were three peak PM_{10} concentrations observed in three target domains, which were 154 μg m^{-3} at the Matsu Islands, 170 μg m^{-3} at the Kinmen Islands, and 60 μg m^{-3} at the Penghu Islands, respectively. On March 6th, 2013, a peak PM_{10} concentration commonly was higher than 110 μg m^{-3} was observed at the Matsu Islands. As illustrated in the weather chart (Fig. S-4(a)), the northern Taiwan Strait including the Matsu Islands and the northern Taiwan

Table 2. Source apportionment of PM_{10} sampled at the island and coastal sampling sites in the Taiwan Strait.

Emission	Spring					Summer					Fall					Winter				
Sources	XM	KM	MT	FZ	PH	XM	KM	MT	FZ	PH	XM	KM	MT	FZ	PH	XM	KM	MT	FZ	PH
Industrial Boilers	17.48	11.94	8.31	10.35	6.31	5.54	6.36	4.73	5.37	2.37	15.76	13.32	4.73	7.51	3.37	16.72	13.11	6.51	7.77	5.37
Petroleum Plants	3.33	3.17	6.91	8.82	4.31	6.89	3.39	3.31	2.05	2.31	6.13	6.37	4.84	7.96	5.77	5.95	5.51	3.7	4.98	3.37
Cement Plants	4.97	2.56	3.37	5.31	1.11	-	2.47	2.2	4.89	0.37	1.04	3.01	2.87	2.83	-	2.56	4.01	2.11	4.27	-
Secondary Nitrate	6.93	5.97	11.43	10.58	8.31	13.71	8.81	9.36	10.03	9.31	9.82	8.57	7.94	8.86	11.53	7.64	7.12	8.73	9.43	9.37
Secondary Sulfate	11.77	10.42	12.03	12.79	13.31	10.76	9.92	10.17	12.83	11.51	10.07	9.05	8.99	9.23	14.37	11.97	13.44	9.83	15.02	12.53
Vehicular Exhausts	19.74	15.45	19.29	20.78	12.33	21.09	15.39	13.22	18.77	15.73	16.16	15.86	12.91	18.62	16.37	9.54	14.53	14.87	19.33	10.37
Oceanic Spray	4.87	5.34	4.75	4.27	10.13	3.12	6.15	15.25	9.59	8.91	3.73	6.5	13.47	8.54	11.35	3.15	5.13	11.78	9.09	12.37
Biomass Burning	4.34	4.67	11.36	12.87	11.71	-	-	4.04	6.28	5.73	3.16	2.59	5.2	2.87	6.73	3.67	6.48	4.55	3.06	7.90
Soil Dusts	19.93	24.51	4.74	9.05	20.55	19.56	23.28	12.52	17.34	24.57	21.2	18.36	22.37	16.69	20.37	24.61	17.62	14.08	16.02	21.33
Steel Plants	5.24	5.86	2.83	3.32	1.11	3.37	6.65	1.94	3.31	-	5.11	3.34	3.81	3.37	-	3.68	0.34	3.33	3.59	-
Others	1.40	10.11	14.98	1.86	10.82	15.96	17.58	23.26	9.54	19.19	7.82	13.03	12.87	13.52	10.14	10.51	12.71	15.32	12.63	17.39
Mass Percentage	98.6	89.89	85.02	98.14	89.18	84.04	82.42	76.74	90.46	80.81	92.18	86.97	87.13	86.48	89.86	89.49	87.29	84.68	87.37	82.61
R^2	0.84	0.87	0.88	0.91	0.88	0.87	0.85	0.87	0.85	0.81	0.81	0.83	0.81	0.80	0.85	0.93	0.93	0.93	0.91	0.88

"-": unresolved; Unit: % (exclude R^2).

Island was covered by the western Pacific subtropical high (WPSH) pressure system. In the early morning of that day, the prevailing wind at the Matsu Islands turned from the northwest to the northeast. An anticyclonic high pressure cold frontal system was observed at the Matsu Islands, resulting in stable atmosphere that restricted the dispersion of air pollutants in the ambient air.

At the Daytime of April 11th, 2014, a peak PM_{10} concentration of 170 μg m^{-3} was observed at the Kinmen islands. The prevailing wind of Domain 2 came from the northeast. A peak PM_{10} concentration appeared at 10:00–11:00 AM of that day whenever the cyclonic circulation phenomenon occurred. It was also observed that the prevailing winds turned gradually from the northeast to the northwest, because a cold high pressure frontal system existed around the Yangtze River Basin, of which the Kinmen Islands are located at the leading edge of the cold frontal system. Under this circumstance, the dispersion of air pollutants in the plenary boundary was inhibited due to the stable atmosphere (Fig. S-4(b)).

On October 8th, 2013, the center of Typhoon Danas was located in the eastern offshore region of the Taiwan Island and moved gradually toward Japan. Under this atmospheric condition, the western bank and the western offshore regions of the Taiwan Island were mainly influenced by leeward effects caused by the peripheral circulation of Typhoon Danas closely contacting the Central Ridge of the Taiwan Island (Fig. S-4(c)). A stable wake pressure zone was observed within this area and the near-surface wind speeds were as low as 1 m sec^{-1}. Hence, the dispersion of air pollutants in the ambient air of the Penghu Islands was unfavorable and caused high PM_{10} concentration as high as 50 μg m^{-3}. As a matter of fact, the PM_{10} concentration was usually very low during these periods. The leeward effects may be the most important factor causing poor ambient air quality at the Penghu Islands.

Fig. 4 illustrates the simulated surface wind fields in three island domains. There were three important features regarding the near surface winds. We selected the highest PM_{10} concentrations observed in the season of spring at different island domains. The air masses came obviously from different directions for these three domains. Fig. 4(a) showed that the air masses moved toward the south due to strong northward winds (Domain 1). The air mass plumes became concentrated at these regions. The results also suggested that high PM_{10} concentrations at the MT and FZ islands were mainly affected by long-range transportation particularly under the calm wind conditions. Fig. 4(b) showed that the surface wind fields were generally dominated by the Northeastern Monsoons in the season of spring in the Kinmen Islands (Domain 2). At the highest PM_{10} concentrations, the wind directions turned from the northeast to the southwest.

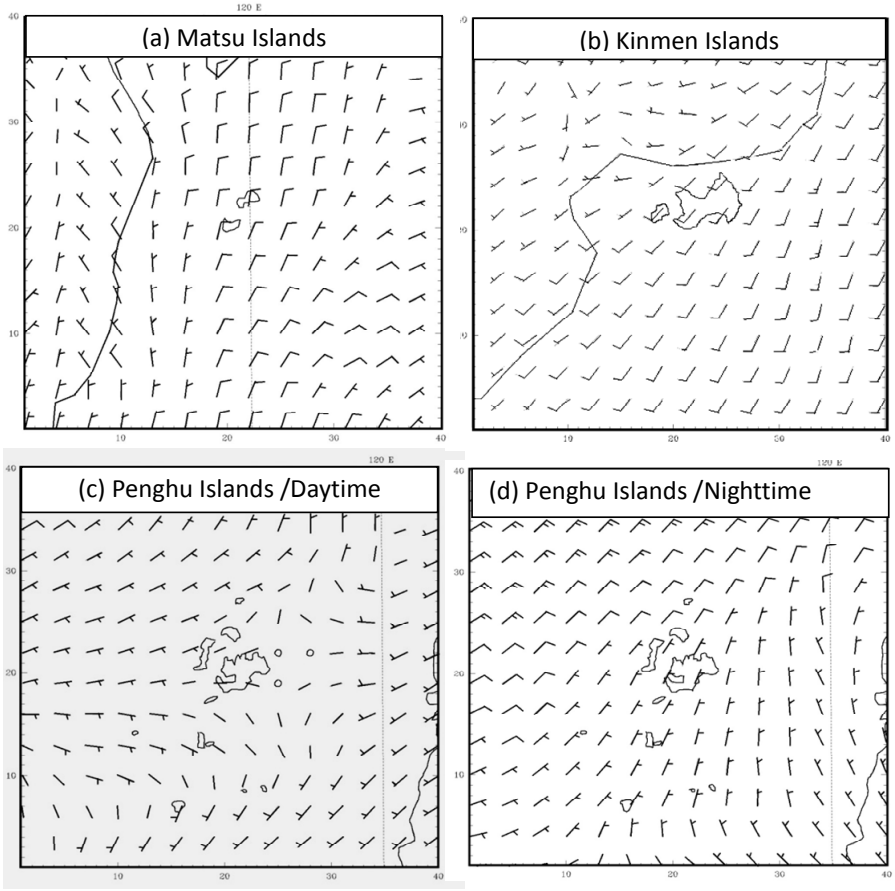

Fig. 4. Simulated surface wind fields at the peak PM_{10} concentration events at the island sampling sites in the Taiwan Strait.

There was a low pressure cyclone system centered at the northwest offshore region of the Kinmen Islands, coupled with the Southwestern Monsoons. A significant cyclonic air circulation was observed in the region. These results indicated that a superimposition phenomenon was observed during the air pollution episodes mainly affected by the combination effects of long-range cross-boundary transportation and local emissions at Xiamen and Kinmen regions. Figs. 4(c) and 4(d) illustrate the surface wind fields at the Penghu Islands (Domain 3) where the surface wind fields varied in the daytime and at nighttime. In the daytime, the air masses were divided into two separate zones. On the west side of the Penghu Islands, a strong northward prevailing wind was coupled with the sea-land breeze, causing by the sea breezes in the southwestern coastal region of the Taiwan Island. Conversely, the surface wind directions moved to the east on the east-side of the Penghu Islands.

CONCLUSIONS

The spatiotemporal distribution, physicochemical characteristics, and source apportionment of PM_{10} sampled at three offshore islands and two relevant coastal regions in the Taiwan Strait were compared. This study revealed that the PM_{10} concentrations were generally higher at the Kinmen and Xiamen domain than other two domains. A superimposition phenomenon was regularly observed at the southwestern Taiwan Strait, indicating that both local emissions and long-range transport were important at the southwestern Taiwan Strait. Long-range transportation from northeastern coastal regions of North mainland China, Korean Peninsula or Japan Islands would affect the ambient atmospheric particle concentration at the northern than those at the southern Taiwan Strait.

Chemical analysis of PM_{10} showed that the most abundant water-soluble ionic species were SO_4^{2-}, NO_3^-, and NH_4^+, suggesting that PM_{10} was mainly composed of secondary ammonium sulfate and ammonium nitrate. Crustal elements (Ca, Mg, Fe, and Al) contributed the major metallic content of PM_{10}, while the concentrations of trace metals (Cd, As, Ni, and Cr) increased during the Northeastern Monsoon periods, showing that Northeastern Monsoons could bring anthropogenic particles with high content of trace metals emitted from diverse sources. The concentrations of OC in PM_{10} at the island sites in the Taiwan Strait were always higher than those of EC for all seasons. The mass ratios of OC to EC (OC/EC) at the sampling sites ranged from 2.0 to 3.0 at the MT, FZ, and PH sampling sites, and from 1.5 to 2.0 at the KM and XM sampling sites, suggested the formation of secondary aerosols was commonly observed in the Taiwan Strait.

The simulated surface wind field showed that the air masses came from different directions for three islands domains. In the Matsu Islands domain, the surface winds came mainly from the north, which blew atmospheric particles from long-range transportation toward the northwestern Taiwan Strait. In the Kinmen Islands domain, high pressure cyclonic systems caused the accumulation of atmospheric particles in the Xiamen Bay from both local sources and long-range transportation, i.e., the superimposition phenomenon. In the Penghu Islands domain, the surface winds in the east-side of the islands coupled with the sea-land breezes resulted in the accumulation of atmospheric particles due to sea-land breeze effects. These results concluded that both prevailing winds and sea-land breezes highly influenced the surface wind fields covering the island and coastal region, which resulted in the superimposition phenomenon of poor air quality causing by the combination of local sources and northward long-range transportation.

ACKNOWLEDGMENTS

This study was performed under the auspices of Environmental Protection Bureaus of Kinmen and Lienchiang Governments. The authors would like to express their great appreciation to NCAR for releasing and updating the WRF chem model. NCEP/NCAR reanalysis data were obtained from NOAA CDC of this work. The meteorological and air quality observation data were supplied by the Data Bank for Atmospheric Research https://dbar.ttfri.narl.org.tw/

SUPPLEMENTARY MATERIALS

Supplementary data associated with this article can be found in the online version at http://www.aaqr.org.

REFERENCES

Appel, B.R., Tokiwa, Y., Haik, M. and Kothny, E.L. (1984) Artifact Particulate Sulfate and Nitrate Formation on Filter Media. *Atmos. Environ.* 18: 409–416.

Borge, R., Alexandrov, V., DelVas, J.J., Lumbreras, J. and Rodriguez, E. (2008). A Comprehensive Sensitivity Analysis of the WRF Model for Air Quality Applications over the Iberian Peninsula. *Atmos. Environ.* 42: 8560–8574.

Cachier, H., Bermond, M.P. and Buat-Menard, P.A.T.R.I.C.K. (1989). Determination of Atmospheric Soot Carbon with a Simple Thermal Method. *Tellus Ser. B* 41: 379–390.

Cadle, S.H. and Groblicki, P.J. (1982). An Evaluation of Methods for the Determination of Organic and Elemental Carbon in Particulate Samples, In *Particulate Carbon Atmospheric Life Cycle*, Wolff, G.T. and Klimisch, R.L. (Eds.), Plenum Press, New York, pp. 89–109.

Chen, F., Hiroyuki, K., Robert, B., Jason, C., Grimmond, C.S.B., Susanne G.C., Thomas, L., Kevin, W.M., Alberto, M., Shiguang, M., David, S., Francisco, P.S., Haider, T., Mukul, T., Xuemei, W., Wyszogrodzki, A.A. and Chaolin, Z. (2011). The Integrated WRF/Urban Modelling System: Development, Evaluation, and Applications to Urban Environmental Problems. *Int. J. Climatol.* 31: 273–288.

Chen, P., Wang, T.J., Hu, X. and Xie, M. (2015). Chemical Mass Balance Source Apportionment of Size-Fractionated Particulate Matter in Nanjing, China. *Aerosol Air Qual. Res.* 15: 1855–1867.

Cheng, M.T. and Tsai, Y.I. (2000). Characterization of

Visibility and Atmospheric Aerosols in Urban, Suburban, and Remote Areas. *Sci. Total Environ*. 263: 101–114.

Chester, R., Nimmo, M., Keyse, S. and Zhang, Z. (2000). Trace Metal Chemistry of Particulate Aerosols from The UK Mainland Coastal Rim Of The NE Irish Sea. *Atmos. Environ*. 34: 949–958.

Feng, Y., Chen, Y., Guo, H., Zhi, G., Xiong, S., Li, J., Sheng, G. and Fu, J. (2009). Characteristics of Organic and Elemental Carbon in $PM_{2.5}$ Samples in Shanghai, China. *Atmos. Res.* 92: 434–442.

Gundel, L.A., Dod, R.L., Rosen, H. and Novakov, T. (1984). The Relationship between Optical Attenuation and Black Carbon concentration for Ambient and Source Particles. *Sci. Total Environ*. 36: 197–202.

Han, L., Zhuang, G., Cheng, S. and Li, J. (2007). The Mineral Aerosol and Its Impact on Urban Pollution Aerosols over Beijing, China. *Atmos. Environ.* 41: 7533–7546.

Hildemann, L.M., Markowski, G.R. and Cass, G.R. (1991). Chemical Composition of Emissions from Urban Sources of fine Organic Aerosol. *Environ. Sci. Technol.* 25: 744–759.

Hsu, S.C., Liu, S.C., Tsai, F., Engling G., Lin, I.I., Chou, C.K.C., Kao, S.J., Lung, S.C.C., Chan, C.Y., Lin S.C., Huang, J.C., Chi, K.H., Chen, W.N., Lin, F.J., Huang, C.H., Kuo C.L., Wu, T.C. and Huang, Y.T. (2010). High Wintertime PM Pollution over an Offshore Island (Kinmen) off Southeastern China: An Overview. *J. Geophys. Res.* 115: D17309, doi: 10.1029/2009JD01364 1.

Hu, W.W., Hu, M., Deng, Z.Q., Xiao, R., Kondo, Y., Takegawa, N., Zhao, Y.J., Guo, S. and Zhang, Y.H. (2012). The Characteristics and Origins of Carbonaceous Aerosol at a Rural Site of PRD in Summer of 2006. *Atmos. Chem. Phys.* 12: 1811–1822.

Huang, X., Olmez, I. and Aras, N.K. (1994). Emissions of Trace Elements from Motor Vehicles: Potential Marker Elements and Source Composition Profile. *Atmos. Environ.* 28: 1385–1391.

Huang, X.X., Wang, T.J., Jiang, F., Liao, J.B., Cai, Y.F., Yin, C.Q., Zhu, J.L. and Han, Y. (2013). Studies on a Severe Dust Storm in East Asia and its Impact on the Air Quality of Nanjing, China. *Aerosol Air Qual. Res.* 13: 179–193.

Khan, B., Hay, M.D., Geron, C. and Jetter, J. (2012). Differences in the OC/EC Ratios that Characterize Ambient and Source Aerosols Due to Thermal-Optical Analysis. *Aerosol Sci. Technol.* 46: 127–137.

Kocak, M., Mihalopoulos, N. and Kubilay, N. (2007). Chemical Composition of the Fine and Coarse Fraction of Aerosols in the Northeastern Mediterranean. *Atmos. Environ.* 41: 7351–7368.

Kothai, P., Saradhi, I.V., Prathibha, P., Hopke, P.K., Pandit, G.G. and Puranik, V.D. (2008). Source Apportionment of Coarse and Fine Particulate Matter at Navi Mumbai, India. *Aerosol Air Qual. Res.* 8: 423–436.

Kumar, R., Naja, M., Pfister, G.G., Barth, M.C., Wiedinmyer, C. and Brasseur, G.P. (2012). Simulations over South Asia Using the Weather Research and Forecasting Model with Chemistry (WRF-Chem): Chemistry Evaluation and Initial Results. *Geosci. Model Dev.* 5: 619–648.

Lavanchy, V.M.H., Gaggeler, H.W., Nyeki, S. and Baltensperger, U. (1999). Elemental Carbon (EC) and Black Carbon (BC) Measurements with a Thermal Method and a Aethalometer at the High-Alpine Research Station Jungfraujoch. *Atmos. Environ.*, 33: 2759–2769.

Lewandowska, A., Falkowska, L., Murawiec, D., Pryputniewicz, D., Burska, D. and Bełdowska, M. (2010). Elemental and Organic Carbon in Aerosols over Urbanized Coastal Region (Southern Baltic Sea, Gdynia). *Sci. Total Environ*. 408: 4761–4769.

Li, T.C., Chen, W.H., Yuan, C.S., Wu, S.P. and Wang, X.H. (2013a). Physicochemical Characteristics and Source Apportionment of Atmospheric Particles in Kinmen-Xiamen Airshed. *Aerosol Air Qual. Res.* 13: 308–323.

Li, T.C., Chen, W.H., Yuan, C.S., Wu, S.P. and Wang, X.H. (2013b). Diurnal Variation and Chemical Characteristics of Atmospheric Aerosol Particles and Their Source Fingerprints at Xiamen Bay. *Aerosol Air Qual. Res.* 13: 596–607.

Lin, C.Y., Liu, S.C., Chou, Charles C.K., Liu, T.H., Lee, C.T., Yuan, C.S., Shiu, C.J. and Young, C.Y. (2004). Long-Range Transport of Asian Dust and Air Pollutants to Taiwan. *Terr. Atmos. Ocean. Sci.* 15: 759–784.

Lin, P., Hu, M., Deng, Z., Slanina, J., Han, S., Kondo, Y., Takegawa, N., Miyazaki, Y., Zhao, Y. and Sugimoto, N. (2009). Seasonal and Diurnal Variation of Organic Carbon in $PM_{2.5}$ in Beijing and the Estimation of Secondary Organic Carbon. *J. Geophys. Res.* 114: D00G11, doi: 10.1029/2008JD010902.

Lin, J.J. (2002). Characterization of the Major Chemical Species in $PM_{2.5}$ in the Kaohsiung City, Taiwan. *Atmos. Environ.* 36: 1911–1920.

Liu, X.D., Chi, X.G., Duan, F.K., Dong, S.P. and Yu, T. (2000). Determination of Organic Carbon and Elemental Carbon in Chinese Urban Aerosols by Using CHN Elemental Analyzer. *J. Aerosol Sci.* 31: S240–S241.

Lo, K.C. and Huang, C.H. (2012). The Development and Application of Weather Research Forecast Chemistry Model. *Int. J. Adv. Computer Technol.* 4: 138–145.

Jen, Y.H., Liu, Y.C., Ie, I.R., Yuan, C.S. and Hung, C.H. (2014). Source Allocation of Long-Range Asian Dusts Transportation across the Taiwan Strait by Innovative Chemical-Assisted Identification Methods. *Adv. Meteorol*. 2014: 268037, doi: 10.1155/2014/268037.

Jiang, F., Wang, T., Wang, T., Xie, M. and Zhao, H. (2008). Numerical Modelling of a Continuous Photochemical Pollution Episode in Hong Kong Using WRF-chem. *Atmos. Environ*. 42: 8717–8727.

Matusik, J. and Kłapyta, Z. (2013) Characterization of Kaolinite Intercalation Compounds with Benzylalkyl Ammonium Chlorides Using XRD, TGA/DTA and CHNS Elemental Analysis. *Appl. Clay Sci.* 433–440.

Millet, D.B., Donahue, N.M., Pandis, S.N., Polidori, A., Stanier, C.O., Turpin B.J. and Goldstein A.H. (2005). Atmospheric Volatile Organic Compound Measurements during the Pittsburgh Air Quality Study: Results, Interpretation, and Quantification of Primary and Secondary Contributions. *J. Geophys. Res.* 110: D07S07,

doi: 10.1029/2004jd004601.

Nriagu, J.O. (1988). A Silent Epidemic of Environmental Metal Poisoning. *Environ. Pollut.* 50: 139–161.

Pathak, R.K., Liou, P.K.K. and Chan, C.K. (2004). Characteristics of Aerosol Acidity in Hong Kong. *Atmos. Environ.* 38: 2965–2974.

Pandis, S.N., Harley, R.A., Cass, G.R. and Seinfeld, J.H. (1992). Secondary Organic Aerosol Formation and Transport. *Atmos. Environ.* 26A: 2269–2282.

Peckham, S.E., Grell, G.A., Mckeen, S.A., Ahmadov, R., Barth, M., Pfister, G., Wiedinmyer, C., Fast, J.D., Gustafson, W.I., Ghan, S.J., Zaveri, R., Easter, R.C., Barnard, J., Chapman, E., Hewson, M., Schmitz, R., Salzmann, M., Beck, V. and Freitas, S.R. (2012). WRF/Chem Version 3.4 User'S Guide. NOAA Earth System Research Laboratory. National Center for Atmosphere Research, Boulder Colorado, USA.

Pirrone, N., Keeler, G.J., Nriagu, J.O. and Warner, P.O. (1996). Historical Trends of Airborne Trace metals in Detroit from 1971 to 1992. *Water Air Soil Pollut.* 88: 145–165.

Shahid, M.Z., Liao, H., Li, J.P., Shahid, I., Lodhi, A. and Mansha, M. (2015). Seasonal Variations of Aerosols in Pakistan: Contributions of Domestic Anthropogenic Emissions and Transboundary Transport. *Aerosol Air Qual. Res.* 15: 1580–1600.

Shi, G.L., Liu, G.R., Peng, X., Wang, Y.N., Tian, Y.Z., Wang, W. and Feng, Y.C. (2014). A Comparison of Multiple Combined Models for Source Apportionment, Including the PCA/MLR-CMB, Unmix-CMB and PMF-CMB Models. *Aerosol Air Qual. Res.* 14: 2040–2050.

Strader, R., Lurmann, F. and Pandis, S.N. (1999). Evaluation of Secondary Organic Aerosol Formation in Winter. *Atmos. Environ.* 33: 4849–4863.

Tsai, H.H., Ti, T.H., Yuan, C.S., Hung, C.H. and Lin, C. (2008). Effects of Sea-Land Breezes on the Spatial and Temporal Distribution of Gaseous Air Pollutants around the Coastal Region of Southern Taiwan. *Environ. Eng. Manage. J.* 18: 387–396.

Tsai, H.H., Yuan, C.S., Hung, C.H. and Lin, Y.C. (2010). Comparing Physicochemical Properties of Ambient Particulate Matter of Hot Spots in a Highly Polluted Air Quality zone. *Aerosol Air Qual. Res.* 10: 331–344.

Tsai, J.H., Huang, K.L., Lin, N.H., Chen, S.J., Lin, T.C., Chen, S.C., Lin, C.C., Hsu, S.C. and Lin, W.Y. (2012). Influence of an Asian Dust Storm and Southeast Asian Biomass Burning on the Characteristics of Seashore Atmospheric Aerosols in Southern Taiwan. *Aerosol Air Qual. Res.* 12: 11105–1115.

Turpin, B.J., Cary, R.A. and Huntzicker, J.J. (1990). An in-Situ, Time-Resolved Analyzed for Aerosol Organic and Elemental Carbon. *Aerosol Sci. Technol.* 12: 161–171.

Turpin, B.J. and Huntzicker, J.J. (1991). Secondary Formation of Organic Aerosol in the Los Angeles Basin: a Descriptive Analysis of Organic and Elemental Carbon Concentrations. *Atmos. Environ.* 25: 207–215.

Turpin, B.J. and Huntzicker, J.J. (1995). Identification of Secondary Organic Aerosol Episodes and Quantification of Primary and Secondary Aerosol Concentrations during SCAQS. *Atmos. Environ.* 29: 3527–3544.

Wang, X.H., Bi, X.H., Sheng, G.Y. and Fu, J.M. (2006). Chemical Composition and Sources of PM_{10} and $PM_{2.5}$ Aerosols in Guangzhou, China. *Environ. Monit. Assess.* 119: 425–439.

Wang, W.C., Chen, K.S., Chem, S.J., Lin, C.C., Tsai, J.H., Lai, C.H. and Wang, S.K. (2008). Characteristics and Receptor Modelling of Atmospheric $PM_{2.5}$ at Urban and Rural Sites in Pingtung. Taiwan. *Aerosol Air Qual. Res.* 8: 112–129.

Witz, S., Eden, R.W., Wadiey, M.W., Dunwoody, C., Papa, R.P. and Torre, K.J. (1990). Rapid Loss of Particulate Nitrate, Chloride and Ammonium on Quartz Fiber Filters during Storage. *J. Air Waste Manage. Assoc.* 40: 53–61.

Wu, S.P., Schwab, J., Yang, B.Y., Zheng, A. and Yuan, C.S. (2015). Two-years $PM_{2.5}$ Observations at Four Urban Sites along the Coast of Southeastern China. *Aerosol Air Qual. Res.*15: 1799–1812.

Yatkin, S. and Bayram, A. (2008). Source Apportionment of PM_{10} and $PM_{2.5}$ Using Positive Matrix Factorization and Chemical Mass Balance in Izmir, Turkey. *Sci. Total Environ.* 390: 109–123.

Yao, X., Lau, P.S., Fang, M., Chan, C.K. and Hu, M. (2003). Size Distributions and Formation of Ionic Species in Atmospheric Particulate Pollutants in Beijing, China: l-Inorganic Ions. *Atmos. Environ.* 37: 2991–3000.

Yuan, C.S., Lee, C.G., Liu, S.H., Yuan, C., Yang, H.Y. and Chen, C.T. (2002). Developing Strategies for Improving Urban Visual Air Quality. *Aerosol Air Qual. Res.* 2: 9–22.

Yuan, C.S., Sau, C.C., Chen, M.C., Hung, M.H., Chang, S.W. and Lin, Y.C. (2004). Mass Concentration and Size-resolved Chemical Composition of Atmospheric Aerosols Sampled at Pescadores Islands during Asian Dust Storm Periods in the Years of 2001 and 2002. *Terr. Atmos. Ocean. Sci.* 15:857–879.

Yuan, C.S., Lee, C.G., Liu, S.H., Chang, J.C., Yuan, C. and Yang, H.Y. (2006). Correlation of Atmospheric Visibility with Chemical Composition of Kaohsiung Aerosols. *Atmos. Res.* 82: 663–679.

Received for review, March 20, 2015
Revised, June 11, 2015
Accepted, June 11, 2015